Communication

Catalytic Synthesis and Structural Characterizations of a Highly Crystalline Polyphenylacetylene Nanobelt Array

Wei Liu, Zhi-Min Cui, Qiang Liu, Dong-Wei Yan, Jing-Yi Wu, Hui-Juan Yan, Yun-Long Guo, Chun-Ru Wang, Wei-Guo Song, Yun-Qi Liu, and Li-Jun Wan

J. Am. Chem. Soc., **2007**, 129 (43), 12922-12923• DOI: 10.1021/ja075540b • Publication Date (Web): 09 October 2007

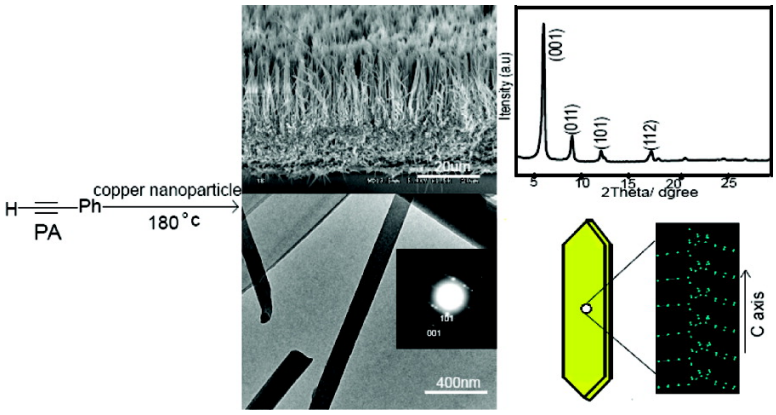

More About This Article

Additional resources and features associated with this article are available within the HTML version:

- Supporting Information
- Links to the 1 articles that cite this article, as of the time of this article download
- Access to high resolution figures
- Links to articles and content related to this article
- Copyright permission to reproduce figures and/or text from this article

View the Full Text HTML

J|A|C|S
COMMUNICATIONS

Published on Web 10/09/2007

Catalytic Synthesis and Structural Characterizations of a Highly Crystalline Polyphenylacetylene Nanobelt Array

Wei Liu,[‡] Zhi-Min Cui,[‡] Qiang Liu,[‡] Dong-Wei Yan,[‡] Jing-Yi Wu,[†] Hui-Juan Yan,[†] Yun-Long Guo,[‡] Chun-Ru Wang,*[,†] Wei-Guo Song,*[,†] Yun-Qi Liu,[†] and Li-Jun Wan[†]

Beijing National Laboratory for Molecular Sciences, Chinese Academy of Sciences, Beijing 100080, China, and Graduate School of Chinese Academy of Sciences, Beijing 100039, China

Received July 24, 2007; E-mail: crwang@iccas.ac.cn; wsong@iccas.ac.cn

One-dimensional nanostructures of conducting polymers such as polyaniline nanofibers,[1−3] polypyrrole nanowires,[4] polydiacetylene nanowires,[5] and polyacetylene nanofibers[6,7] have been extensively studied in recent years. Since the devices made of organic single crystals have shown outstanding optical and electronic performances,[8,9] it is highly interesting to study whether single crystalline conducting polymers, especially the conjugated polymers, also show such properties. Polyphenylacetylene (PPA) is an aryl-substituted conjugated polymer with excellent stability in air and has many potential applications in gas-selective permeable membranes, magnetic, liquid crystalline, and nonlinear optical materials,[10] so we choose the single crystalline PPA as a typical conducting polymer to study its synthesis, structural characterizations, and transistor performance.

Conventional synthesis method for PPA is through polymerization of phenylacetylene in the liquid phase with an organorhodium catalyst.[11] In this communication, we adopt a new approach to synthesize PPA nanobelts in the gas phase by using the nanocopper particles as catalyst. The PPA produced by this method shows single crystalline structure and owns specific cis-phase conformation. Moreover, this synthetic route has other advantages compared to the conventional method; for example, it uses copper catalyst to avoid those expensive noble metals and it uses the gas-phase reaction to avoid the use of toxic organic solvents.

In a typical experiment, 50 mg of copper nanoparticles (average size 100 nm) was transferred into a 50 mL Teflon-lined stainless steel autoclave, which was purged with argon for 20 min, then 0.25 mL of phenylacetylene (PA, Alfa Aesar) was added into the autoclave. The autoclave was sealed and heated to 180 °C, maintaining the high temperature for certain times, and was then cooled to room temperature. A self-supported disc-like yellowish piece was obtained and characterized as a PPA nanobelt array as shown later.

The boiling point of PA is only 142 °C, so at 180 °C, the PA molecules were readily vaporized and were polymerized with the catalysis of copper nanoparticles. The Cu catalyst plays a key role in the PA polymerization reaction. Previous reports have shown that PA could be thermally polymerized at temperatures of 120 °C or above.[12] However, our control experiments revealed that, without copper particles, only viscous liquid was produced even under high temperature at 300 °C.

The as-prepared PPA was studied by the scanning electron microscope (SEM) as shown in Figure 1a−c. PPA forms a vertically well-aligned nanobelt array, which grows nearly vertically from a ca. 20 μm thick dense layer, as shown in Figure 1b. The EDS analysis of the dense layer (inset in Figure 1b) indicates that, besides a trace of oxygen contributed from the residue copper oxide in the copper catalyst, only carbon and Cu are found. Further SEM study (Figure S2) revealed that the dense layer is composed of some tight-bundled PPA nanobelts, which wrap the nanocopper particles tightly.

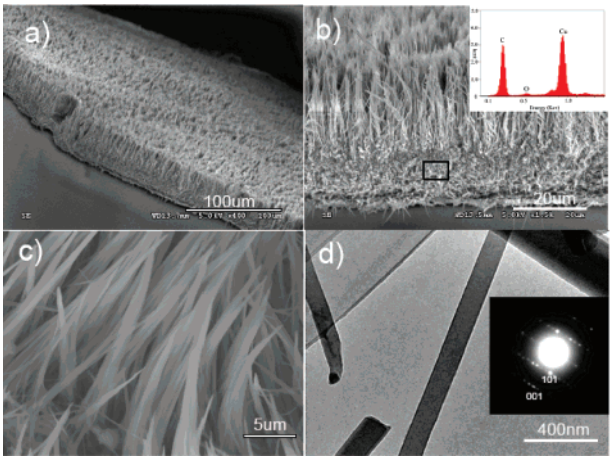

Figure 1. (a) SEM image of the overall PPA array. (b) Cross-sectional SEM view of the PPA array and the dense layer below. Inset is the EDS spectrum for the circled area. (c) High-resolution SEM image of the PPA nanobelt array. (d) TEM study of a single PPA nanobelt; inset shows the selected area electron diffraction (SAED) pattern.

The growth mechanism of the PPA array can be explained by a vapor−solid model. At the beginning of PA reactions, naked copper nanoparticles are exposed to the PA vapor and catalyze the PA polymerizing reaction to form PPA nanobelts quickly. However, as the reaction continues, the PPA belts wrap the catalyst particles and gradually form a dense layer of PPA belts that effectively reduce the access of PA vapor to the catalysts, so the PA polymerizing reaction is slowed and a sparse PPA nanobelt array begins to form above the dense layer of PPA, as shown in Figure 1b. The high-magnification SEM in Figure 1c shows partial PPA arrays that are composed of a hundred PPA nanobelts with uniform size and similar morphology.

The structural details of PPA nanobelts were further characterized by TEM, AFM, and XRD. As shown in Figures 1 and S3, the TEM and AFM images of the nanobelt indicate that the typical size of an individual PPA nanobelt is ca. 135 nm (width) × 24 nm (thickness) × 20 μm (length). The selected area electron diffraction (SAED) pattern (inset in Figure 1d) indicated that the nanobelts have single crystalline structure growing along the *c*-axis (Figure 2b). This conclusion is further supported by the XRD study of the PPA sample (Figure 2a). The strong and sharp XRD signals suggest the highly crystalline structure of PPA nanobelts, and the main peak at 5.98° corresponds to the preferential [001] growth face of the PPA single crystal.

[†] Beijing National Laboratory for Molecular Sciences, Chinese Academy of Sciences.
[‡] Graduate School of Chinese Academy of Sciences.

10.1021/ja075540b CCC: $37.00

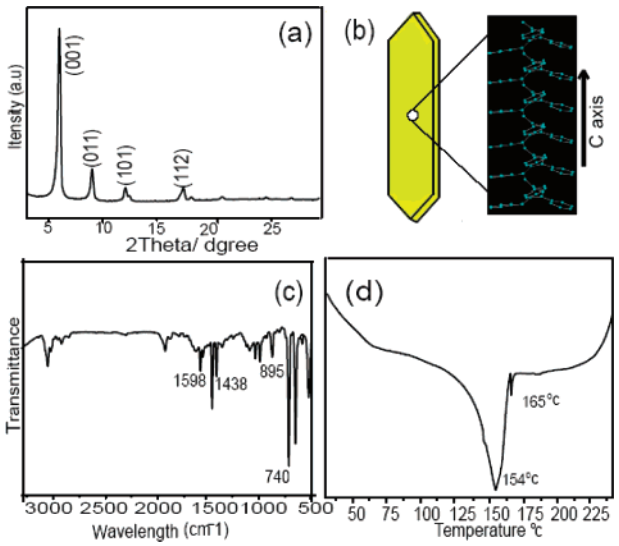

Figure 2. (a) XRD pattern of the PPA nanobelt array. (b) Structural model of the cis-PPA molecular chains. (c) IR spectrum of the PPA nanobelts. (d) DSC melting curve of the PPA nanobelts.

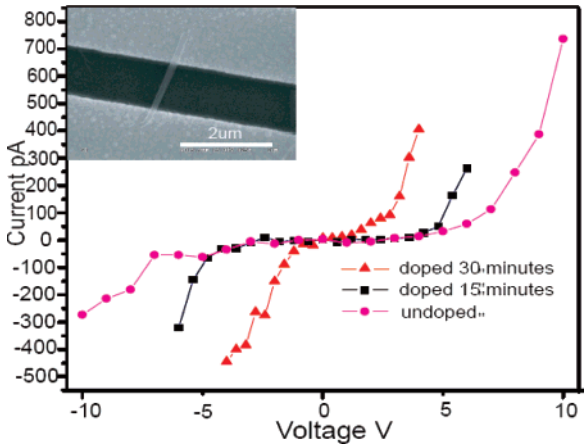

Figure 3. *I*−*V* characteristics of the PPA nanobelts. Inset shows a SEM image of a PPA nanobelt bridging two electrodes.

Single crystalline PPA nanobelts have two possible stereoisomers: cis and trans conformations; and the stereoregularity can be easily assigned with the IR spectrometry by their fingerprint absorption bands at 740 and 760 cm^{-1} for the cis and trans PPA, respectively.[13] The IR spectrum of PPA nanobelts was measured and is shown in Figure 2c, in which the main 740 cm^{-1} peak and a negligible shoulder at ca. 760 cm^{-1} strongly suggest that the as-prepared PPA nanobelts are cis-specific. Thermal analysis of the PPA nanobelts by differential scanning calorimetry (DSC, Figure 2d) shows a melting point at 154 °C and a small sharp peak at 165 °C, separately corresponding to melting points of the cis and the trans phases of the PPA nanobelts. The large difference between the two peaks' areas further confirms the cis-specific property of the PPA nanobelts.

The as-prepared PPA nanobelt array can be easily dispersed into an individual nanobelt and can be individually manipulated. This property is very important for semiconductor applications. In our preliminary efforts to study the properties of the PPA nanobelts, we carefully pressed a single PPA nanobelt onto two 1 μm spaced Au electrodes (inset of Figure 3) to measure its current−voltage characteristics. As shown in Figure 3, a single PPA nanobelt shows good semiconductivity with a wide band gap.

Chemical doping is usually used to tune the transistor property of conducting polymers,[14] so we thus prepared dozens of individual PPA nanobelts to examine their semiconductivity changes after iodine dopings. As previously reported on bulk PPA,[15] the iodine doping of nanobelts dramatically changes the PPA semiconductivity. Three PPA nanobelts were prepared and measured. One was the as-prepared belt (undoped), and the other two nanobelts were in situ doped with iodine vapor for 15 and 30 min, respectively; Figure 3 shows the measured *I*−*V* curves of these three PPA nanobelts. Iodine doping substantially reduces the band gap of PPA semiconductors and increases the belt conductivity in the ohmic region. The belt that underwent 30 min of iodine doping is nearly a conductor, and the conductivity was about 4.8×10^{-4} S/cm in the ohmic region, which is higher than that of the iodine-doped PPA film with similar iodine loading.[15]

In summary, nanocopper particles are excellent catalysts for the stereospecific polymerization of PA to produce cis-specific and highly crystalline PPA. Well-aligned PPA nanobelt arrays are produced through a mild and template-free route. Single PPA nanobelts show semiconductor features, suggesting promising potentials in nanodevice applications. The applications of the PPA nanobelt arrays in sensors, photovoltaic cells, light-emitting display devices, field emission devices, etc., are being explored.

Acknowledgment. This work is supported by The Natural Science Foundation of China (NSFC 20121301, 21573121, and 20673125) and the Major State Basic Research Program of China "Fundamental Investigation on Micro-Nano Sensors and Systems based on BNI Fusion" (Grant 2006CB300402). The authors thank Professors Lin Li and Professor Shou-Ke Yan for valuable discussions.

Supporting Information Available: Experimental details of preparing nanocopper particles; SEM characterization of dense layer and the nanobelts; and the AFM image of the nanobelt. This material is available free of charge via the Internet at http://pubs.acs.org.

References

(1) Wu, C. G.; Bein, T. *Science* **1994**, *264*, 1757.
(2) Jia, X. H.; Richard, B. K. *J. Am. Chem. Soc.* **2004**, *126*, 851.
(3) Xin, Y. Z.; Warren, J. G.; Sanjeev, K. M. *J. Am. Chem. Soc.* **2004**, *126*, 4502.
(4) Yun, M.; Myung, N. V.; Vasquez, R. P.; Lee, C.; Menke, E.; Penner, R. M. *Nano Lett.* **2004**, *4*, 419.
(5) Hai, Y. G.; Hui, B. L.; Yong, J. L.; Qing, Z.; Yu, L. L.; Shu, W.; Tong, G. J.; Ning, W.; Xiao, R. H.; Da, P. Y.; Dao, B. Z. *J. Am. Chem. Soc.* **2005**, *127*, 12452.
(6) Hyun, J. L.; Zhao, X. J.; Andrey, N. A.; Ju, Y. L.; Mun, J. G.; Kazuo, A.; Young, S. K.; Dong, W. K.; Yung, W. P. *J. Am. Chem. Soc.* **2004**, *126*, 16722.
(7) McGehee, M. D.; Heeger, A. J. *Adv. Mater.* **2000**, *12*, 1655.
(8) Alejandro, L. B.; Stefan, C. B. M.; Mang, M. L.; Shu, H. L.; Ricky, J. T.; Colin, R.; Mark, E. R.; Yang, Y.; Fred, W.; Zhen, N. B. *Nature* **2006**, *444*, 913.
(9) (a) Liu, H.; Li, Y.; Xiao, S.; Gan, H.; Jiu, T.; Li, H.; Jiang, L.; Zhu, D.; Yu, D.; Xiang, B.; Chen, Y. *J. Am. Chem. Soc.* **2003**, *125*, 10794. (b) Liu, H.; Zhao, Q.; Li, Y.; Liu, Y.; Lu, F.; Zhuang, J.; Wang, S.; Jiang, L.; Zhu, D.; Yu, D.; Chi, L. *J. Am. Chem. Soc.* **2005**, *127*, 1120.
(10) Chien, J. C. W. *Polyacetylene: Chemistry, Physics, and Material Science*; Academic Press: Orlando, FL, 1984.
(11) Kang, H. P.; Kwonho, J.; Seung, U. S.; Dwight, A. S. *J. Am. Chem. Soc.* **2006**, *128*, 8740.
(12) Ehrlich, P.; R, J. K.; Pierron, E. D.; Provder, T. *Polym. Lett.* **1967**, *5*, 911.
(13) Hisao, H.; Christian, S.; Walter, L. *Appl. Organomet. Chem.* **2001**, *15*, 145.
(14) (a) MacDiarmid, A. G. *Rev. Mod. Phys.* **2001**, *73*, 713. (b) Heeger, A. J. *Rev. Mod. Phys.* **2001**, *73*, 701. (c) Shirakawa, H. *Rev. Mod. Phys.* **2001**, *73*, 713.
(15) Kang, E. T.; Bhatt, A. P.; Villaroe, I. E.; Aderson, W. A.; Ebrlich, P. J. *Polym. Sci. Polym.* **1982**, *20*, 143.

JA075540B